Estimating Planetary Boundary Layer Heights from NOAA Profiler Network Wind Profiler Data

A. Molod[1]
NASA/Goddard Space Flight Center, Greenbelt, MD 20771

H. Salmun[2]
Hunter College of the City Univ. of New York, New York, NY 10065

M. Dempsey
Earth and Environmental Science Doctoral Program, The Graduate Center of CUNY
New York, NY 10016

[1] Additional affiliation: Earth System Science Interdisciplinary Center, Univ. of MD, College Park, MD 20440.
[2] Additional affiliation: Earth and Environmental Science Doctoral Program, The Graduate Center of CUNY, New York, NY 10016.
Corresponding author: Andrea Molod, email: andrea.molod@nasa.gov

Abstract

An algorithm was developed to estimate planetary boundary layer (PBL) heights from hourly archived wind profiler data from the NOAA Profiler Network (NPN) sites located throughout the central United States. Unlike previous studies, the present algorithm has been applied to a long record of publicly available wind profiler signal backscatter data. Under clear conditions, summertime averaged hourly time series of PBL heights compare well with Richardson-number based estimates at the few NPN stations with hourly temperature measurements. Comparisons with clear sky reanalysis based estimates show that the wind profiler PBL heights are lower by approximately 250-500 m. The geographical distribution of daily maximum PBL heights corresponds well with the expected distribution based on patterns of surface temperature and soil moisture. Wind profiler PBL heights were also estimated under mostly cloudy conditions, and are generally higher than both the Richardson number based and reanalysis PBL heights, resulting in a smaller clear-cloudy condition difference. The algorithm presented here was shown to provide a reliable summertime climatology of daytime hourly PBL heights throughout the central United States.

Introduction

The planetary boundary layer (PBL) is the shallow layer of the troposphere nearest to the Earth's surface that, particularly over land, exhibits a diurnal variation due to the exchange of energy and momentum between the surface and the atmosphere. The depth of the PBL can range from less than one hundred meters to several kilometers. Knowledge of the PBL depth and its fluctuations in time are also essential for the estimation of the transport of atmospheric constituents, and in particular to estimate the terms in the atmospheric carbon budget (Denning et al. 2011).

Many methods exist for measuring the PBL depth, including the use of radiosondes (Seidel at al. 2010; Liu and Liang 2010), aircraft (Spangler and Dirks 1974), sodar (Beyrich 1997), wind profilers (Angevine et al. 1994), lidar (Lammert and Bösenberg 2006; Lewis et al. 2012) and Global Positioning System (GPS) radio occultation (Guo et al. 2011; Ao et al. 2012). Each of these methods comes with its own advantages and limitations, so the best option is to use some combination of methods (Seibert et al. 2000). For instance, radiosonde ascents, while performed operationally in numerous locations across the world, are generally limited to twice per day. Aircraft sampling provides spatial information that is useful, but is generally limited to particular regions or specific campaigns and is quite expensive. Lidar has a very high sampling rate, but is limited in that it cannot remain unattended for long periods of time. Wind profilers are quite useful for measuring PBL depths because they can be left unattended for extended time periods, can provide a continuous stream of data over time, and there is an extensive network of operational wind profiler stations in some regions of the world. Wind profilers are, however, limited by the fact that there is generally no sampling below 500 m above the earth's surface.

In addition to the large variety of instruments to measure PBL depth, there is also a large variety of algorithms used to determine the PBL depth. In addition, the physical quantity being measured may vary depending on the measurement method. Even for a single instrument, there are multiple ways to determine the PBL depth. For example, lidar-derived PBL depths have been obtained from gradients or variance in the backscatter profile, wavelet covariance, and fits to idealized profiles (Hooper and Eloranta 1986; Flamant et al. 1997; Steyn et al. 1999; Davis et al. 2000).

One of the earliest successful algorithm to compute PBL height using wind profiler signal to noise ratio (SNR) measurements was developed by Angevine et al. (1994). Their algorithm was tested using data from a site in Alabama during June 1992. They determined the column maximum SNR every six minutes and took the median of these values for the half hour before and after a given hour and used the median as the height of the PBL. The median was used instead of the mean so as not to give outliers any great emphasis. The algorithm included a technique to remove spurious high values of SNR due to ground clutter.

Bianco and Wilczak (2002) developed a PBL height algorithm using wind profiler SNR that was designed to improve on the shortcomings of the algorithm of Angevine et al. (1994). They developed a fuzzy logic algorithm to improve on the elimination of ground clutter and another fuzzy logic algorithm to determine the depth of PBL. The second algorithm uses measures of the peak, gradient, curvature and variance of the hourly median SNR profile along with the variance of the vertical velocity. The fuzzy logic functions were developed using data from a site in California, and tested against data from a site near Houston, TX. The fuzzy logic algorithm showed marked improvements relative to Angevine et al. (1994), particularly in the early morning hours.

Bianco et al. (2008) improved on Bianco and Wilczak (2002)'s methodology for selecting PBL heights by modifying the fuzzy logic algorithm to eliminate ground clutter, and by utilizing the Doppler spectral width to clarify which of multiple maxima in the profile of SNRs correspond to the PBL height. The Doppler spectral width is sensitive to small-scale turbulent fluctuations and was used to detect the presence of an entrainment zone near the top of a growing boundary layer. The modified algorithm was applied to both clear and cloudy boundary layers at sites in Pittsburgh, PA and Plymouth, MA, and was shown to improve PBL estimates on clear days relative to a subjective PBL height determination, but did not perform as well on cloudy days. Heo et al. (2003) also addressed the issue of multiple maxima utilizing the Doppler spectral width.

The covariance wavelet transform (CWT) method, previously used for estimating PBL heights from lidar data (Cohn and Angevine, 2000 and Lewis et al., 2013), was used by Compton et al. (2013) to estimate PBL heights from wind profiler data collected near Beltsville, MD during July 2011. Their results showed that the CWT method can successfully determine PBL height as compared to radiosonde and lidar PBL height estimates, although some special treatment of early morning SNR data was needed to avoid spurious PBL heights.

In the present study, a new algorithm using archived wind profiler signal data to estimate PBL heights is presented. Data are from the NOAA Profiler Network (NPN) sites located mostly throughout the central United States. Our study uses data from approximately 30 NPN stations during the months of June, July and August of 2000 through 2005. The new algorithm relies on the existence of publicly available backscatter signal data (SNR is not archived), is relatively simple and therefore not site-specific and potentially more robust. Following this introduction, Section 2 describes the various data sources used to develop, test and validate the algorithm to estimate PBL heights, and section 3 describes in detail the algorithm developed here. An analysis of the algorithm’s performance and results under clear and mostly cloudy conditions is discussed in Section 4, and the study and results are summarized in section 5.

2. Data for PBL Height estimation and validation

2a. Wind Profilers

Wind profiler data were obtained from the NOAA Profiler Network (NPN) archive site (http://www.profiler.noaa.gov/npn/index.jsp). The majority of the NPN stations are in the central United States, and our study is restricted to that region. The locations of the 31 stations in the study region are marked on Figure 1. Our study period is June, July and August of the years 2000 through 2005. The wind profilers that are part of the NPN are ultra high frequency (UHF) active remote sensing Doppler radars, operating in a frequency range (404 MHz in general, one instrument at 449 MHz). The NPN wind profilers operate with range gates spaced 250 m apart in the vertical, beginning 500 m above the surface. The profilers record backscatter and signal to noise ratios every 6 minutes, but the archive consists of hourly averages of the signal backscatter only.

In the frequency range at which the profilers transmit, the signal is undergoing Bragg scatter, essentially responding to changes in atmospheric density. These density changes are caused by changes in water vapor, temperature, aerosol or hydrometeor content. Changes in atmospheric aerosol, water vapor or temperature with height are sharpest near the top of the planetary boundary layer, and so the wind profiler data may be used to detect boundary layer height.

The limitations of wind profiler data were addressed in a technical report provided by the Federal Coordinator for Meteorological Service and Supporting Research 1998 (FCM-R14-1998). UHF wind profilers are limited in that they must assume a local horizontal uniformity. An example of problems related to inhomogeneous terrain will be shown in section 4. Two other issues related to wind profiler data are contamination from migrating birds and insect swarms, which may flood the signal return. In addition, because of potential interference with the receivers on the six polar-orbiting satellites, the wind profiler's transmitter shuts down for 6 minutes during satellite overpasses. This occurs about 7 times daily (varying between 4 and 10 times) for each site in the network. One of the most significant limitations for the use of wind profiler data to compute PBL heights is the inability to gather data between the surface and

500 m, and therefore precludes the ability to measure nocturnal PBL heights. Despite these limitations, wind profiler data may be used to provide long-term hourly time series of daytime PBL heights.

2b. Additional data for the Algorithm and its Validation

Twelve of the wind profiler sites are equipped with Radio Acoustic Sounder System (RASS) instruments. RASS-based profiles of virtual temperature are provided in the NPN archive, and are used in this study along with the retrieved wind profiles from the profilers to estimate a Richardson-number based PBL height, which will be described in the next section. The RASS virtual temperature retrieval algorithm is based on the sensitivity of the speed of sound to temperature. The RASS instruments emit acoustic energy and measure the speed of the sound waves as they propagate up through the atmosphere (Singal and Goel, 1997).

The analysis of PBL heights includes distinctions between clear and cloudy days. Cloud cover at the NPN sites was determined based on data from the International Satellite Cloud Climatology Project (ISCCP) D1 data (Rossow et al., 1996), which is a global gridded cloud product with a resolution of 290 km^2 at 3-hour intervals. For this study we used the cloud cover percentages (number of cloudy pixels/total number of pixels times 100) for the grid square closest to a given NPN station. ISCCP data were chosen for the determination of cloud cover due to the availability of high temporal resolution data during the time span of NPN data.

Reanalysis estimates of PBL height for comparison with wind profiler estimates were obtained from the Modern-Era Retrospective Analysis for Research and Applications (MERRA, Rienecker et al. 2011) two-dimensional surface turbulent flux dataset (tavg1_2d_flx_Nx). Files were obtained from the NASA/Goddard MDISC (http://disc.sci.gsfc.nasa.gov/mdisc/data-holdings). These data are available hourly, at a spatial resolution of 0.667º in longitude and 0.5º in latitude. MERRA PBL heights are diagnosed by the turbulence parameterization in the underlying atmospheric general circulation model based on the eddy diffusivity coefficient for heat. The PBL height is diagnosed as the level at which the coefficients drop below a value of 2 m s^{-2}. Clear sky daily maximum MERRA PBL heights were shown to be generally lower than satellite based Cloud-Aerosol Lidar and Infrared Pathfinder Satellite Observation (CALIPSO) estimates over tropical oceans (Jordan et al. 2010), and shown to be relatively consistent with CALIPSO over land (McGrath-Spangler et al. 2012).

3. Estimation of PBL Height

The algorithm for estimating PBL heights from wind profiler (WP) data was initially developed for clear sky conditions and refined using data from a station for which RASS temperature measurements were available. Cloud cover was determined using the ISCCP data at the grid point containing the station under examination, and clear days were selected based on the condition that at 10AM, 1PM and 4PM (local time) there was 0% cloud cover. The initial step of the algorithm, and a unique feature of the algorithm developed in this study, consists of determining the time of day at which the PBL rises from its nocturnal value into the range of instrument detection at 500 m above the ground. This step of the algorithm serves the role served by complex elements (e.g., Bianco et al., 2008) or specific limits (Compton et al., 2013) that are present in many algorithms to deal with the noisy morning SNR profiles that are measured when the PBL height is below instrument range. The underlying assumption for the algorithm developed here as well as most lidar or wind profiler PBL height algorithms is that the gradients of moisture, hydrometeors or particles at or near the PBL height will be manifest as maxima in the signal backscatter at the detector. The time at which the PBL height emerges into the instrument's range is therefore the time at which the signal backscatter at the 500 m level is at its daily maximum. Once this "emergence time" is established, the vertical profile of signal backscatter is examined at each subsequent hour to determine the wind profiler (WP) PBL height. If only one local maximum exists for a given hour's profile, the PBL height is assigned to the height of that maximum. If multiple local maxima exist, as was the case for the vast majority of profiles examined, the standard deviation of the column backscatter (up to the level of the largest local maximum) is used to choose which among the local maxima is the "true maximum", and the PBL height is assigned to the height of that "true maximum". Starting from the lowest height at which a local signal maximum exists, each maximum is evaluated against the local minimum above it using the column standard deviation to determine whether it is a "true maximum" or a small "wiggle" in the profile and therefore not the PBL. Any signal maximum value not larger than the minimum above it by more than 1 standard deviation is deemed a "wiggle" and the process of evaluating local maxima proceeds upwards in the column. If a "true maximum" is found, the PBL height is assigned to the height of that maximum, if none is found the algorithm does not return a value for the WP PBL height.

PBL heights were also estimated at the NPN stations with RASS instruments (8 of the stations) using the retrieved virtual temperature profiles and the retrieved wind profiles in the NPN archive. The temperature and wind fields were used to compute a bulk Richardson number (Ri_b) based PBL height estimate after Seidel et al. (2010). The bulk Richardson, Ri_b, number used is given by:

$$Ri_b = \frac{(\frac{g}{\theta_{vs}})(\theta_{vz} - \theta_{vs})(z - z_s)}{u_z^2 + v_z^2},$$

where g is gravity, θ_v is the virtual potential temperature, u and v are the horizontal wind components, and z is height. The subscript s denotes the surface and the surface winds are assumed zero. This bulk Richardson number is evaluated based on differences between the surface and successively higher heights, assuming that the surface layer is unstable, and the PBL top is identified as the level at which Ri_b exceeds a critical value of 0.25. This additional quasi-independent estimate of PBL height was used for validation purposes during the algorithm development and for comparison afterwards. Seidel at al. (2010) found that this Ri_b PBL height algorithm outperformed a θ_v gradient algorithm such as the one used in Bianco and Wilczak (2002) for validation.

An example of the correspondence between the PBL height selected by the WP algorithm and the vertical profiles of the wind profiler backscatter is shown in Figure 2, based on data for Station 74541 (Havilland, KS) on July 4, 2003. The co-location of the maximum in the contours of signal strength with the PBL height (black stars) at each time of day is depicted in figure 2a and demonstrates the general behavior of the algorithm developed here. In this example, the PBL height rises above 500 m in the late morning; it reaches the daytime maximum of approximately 2000 m in the late afternoon and remains there until 7PM local time. The existence of elevated PBL heights late in the afternoon is to be expected based on the response of the wind profiler to aerosol/hydrometeor loads, which on a clear day essentially measures the height of an "aerosol boundary layer". Similar behavior of the diurnal cycle was found by Angevine et al. (1994) using wind profiler SNR at a location in Alabama, by Cohn and Angevine (2000) at a location near Champagne, IL. and by Lewis et al. (2013) at a location in Beltsville, MD. Figure 2b shows the vertical profiles of the wind profiler backscatter up to a height of 4000 m for every hour starting at 1PM local time. Figure 2b shows clearly that at each time of day there are multiple maxima in the profiles, and the ability to distinguish between them is an important element of the algorithm.

4. Results and Discussion

The WP PBL height algorithm was applied to all available data from the stations shown in Figure 1, for the months of June, July and August of 2000 through 2005.Only data with a "0" quality control flag were considered. Comparisons were made to PBL height estimates obtained using the Richardson-number based calculation described in Section 3 and to the PBL heights from MERRA, which are model-based estimates using observationally constrained atmospheric profiles. An example of an individual station's full time series is shown in Figure 3 for illustration, but the focus of the results to be presented is on mean diurnal cycles for each station and for each PBL height estimate (WP, Ri_b and MERRA) under both clear and mostly cloudy conditions. The mean diurnal cycle is computed as the average at each time of day over all clear (or cloudy) days in the study's time span. The time span was adequate to provide at least 10 days in each category for the calculation of the mean diurnal cycle.

An example of a PBL height time series for all the clear days at the Havilland, KS station during June, July and August of 2000 through 2005 is shown in Figure 3. The time series curves in Figures 3a and 3b represent the PBL evolution over a series of juxtaposed 10-hour segments from 10PM to 7PM on a series of clear days for the WP, $R\mathrm{i}_b$ and MERRA estimates. The station-derived (Figure 3a) clear sky determination is based on ISCCP data, and the MERRA determination (Figure 3b) uses its own estimate of cloud fraction and thus is represented by a different sample of days. The daily maxima of the WP and MERRA PBL heights range between 2000 m and 3000 m, with MERRA PBL heights occasionally reaching values up to 3500 m. The daily maximum of the Richardson-number based PBL height is slightly lower and ranges between 1500 m and 2500 m. The clear day mean diurnal cycle for the station in Figures 3a and 3b is shown in Figure 3c. In this example, the mean diurnal cycle of the WP and $R\mathrm{i}_b$ PBL heights are very similar throughout the day and both estimates are lower than the MERRA PBL heights.

As was mentioned in section 2a, inhomogeneous terrain surrounding wind profiler stations may present problems for use of wind profiler data. A map of the terrain variance at scales less than 3 km in the study region (Figure 4a) indicates that New Mexico, Wyoming and Colorado are characterized by large topographic variations of the kind that may interfere with the use of wind profiler backscatter data to determine PBL heights. An example of the typical behavior of the WP algorithm over the station in White Sands, NM, is shown in Figures 4b and 4c. The signal backscatter decreases with height up to approximately 1750 m at all times of the day, and then above that level increases to a local maximum at approximately 2250 m. This behavior makes it difficult to subjectively determine a PBL height "by eye", and in practice the step in the algorithm that searches for a PBL emergence time fails. This behavior is typical for the stations in New Mexico, Colorado and Wyoming, and for this reason they are removed from the analysis of the WP PBL heights to be presented in the remainder of Section 4.

Another type of issue with the WP PBL height algorithm at particular stations is demonstrated in Figure 5, in which the signal backscatter (Figures 5a and 5c) and line plots at two individual times (Figures 5b and 5d) are shown from the station in Lathrop, MO on a clear day, July 21, 2002, and on a cloudy day, August 9, 2002. In the clear day example shown here, the backscatter signal maximum occurs at a level that grows (unreasonably) rapidly in the morning hours, from 750 m to 2000 m in the span of an hour, remains constant at 2000 m at all times of day after 12 Noon, and rises to 2700 m at 7 PM. In the cloudy sky example, the rapid growth is from 500 m to 1750 m in the span of an hour, rising to 2000 m soon afterwards and remaining at 2000 m throughout the day. This pattern of behavior occurs at many clear and cloudy days during the study period, at the station depicted in Figure 5 and at the nearby station in Wolcott, IN (station ID 74466), and determines the behavior of the mean WP PBL height diurnal cycle under clear and cloudy conditions at those two stations. An aerosol layer advected into the range of the station could potentially cause such behavior, but due to the unusual pattern of signal backscatter these two stations are also excluded from the analysis in this section.

4a. Clear Sky PBL Heights

The mean diurnal cycles under clear sky conditions for the seven remaining stations with RASS data are shown in Figure 6. In general throughout the morning and the early afternoon the estimates of PBL height from the WP algorithm (red) and from the Ri_b algorithm (green) are in close agreement and lie below the MERRA PBL heights (blue). In the late afternoon, the WP PBL heights lay between the Ri_b and MERRA PBL heights, as the Ri_b PBL heights drop in many cases and the WP PBL heights generally remain elevated. In addition, the rate of morning PBL height growth is similar among all three PBL height estimates. This characterization of the relationship among the clear sky mean diurnal cycles of the WP, Ri_b and MERRA PBL heights also holds for the stations without RASS instruments.

The seasonal mean clear sky WP PBL heights at station 74546 (Hillsboro, KS, Figure 6c) are comparable in magnitude and diurnal cycle to the PBL height estimates of Liu and Liang (2010) using radiosonde profiles at the nearby Atmospheric Radiation Measurement Southern Great Plains (ARM SGP) site. The median radiosonde-derived PBL heights during June, July and August reach a daily maximum of approximately 1700 m just after 3PM local time, remain elevated until 6PM, and then drop quickly. The WP PBL heights seen in figure 6c also reach a daily maximum of approximately 1700 m at approximately 4PM and remain elevated for the remainder of the day. The Ri_b PBL heights are lower (maximum of 1200 m), and the MERRA PBL heights are higher (near 2000 m).

Figure 7 shows the geographical distribution of the daily maximum clear sky PBL heights from the WP and MERRA estimates at all the wind profiler stations in the study region. The WP PBL heights are highest at the stations located to the west and south and decrease eastward and northward. This pattern generally follows the expected dependence of PBL height on surface temperature and moisture, where the higher PBL heights are found in the warmer and drier areas to the west and south, and lower PBL heights are found in the cooler and moister areas to the north and east. The pattern of MERRA PBL heights is quite different, with large PBL heights in the center of the region. In general, as was seen in Figure 6 at the RASS stations, MERRA PBL heights are higher than WP PBL heights. The warm summertime bias in MERRA surface temperatures in the Great Plains (Bosilovich, 2013) would suggest that MERRA PBL heights are biased high. The warm MERRA surface temperatures along with the agreement between WP PBL heights and the ARM SGP estimates of Liu and Liang (2010) support the credibility of the WP PBL height estimates. The daily maximum PBL height at the station in Winchester, IL (station ID 74556) is approximately 1500 m in both the WP and MERRA estimates. These values are in good agreement with the daily maximum PBL height estimates under clear conditions obtained by Angevine et al. (1998) and by Cohn and Angevine (2000) as part of the Flatlands 1995 and 1996 experiments in nearby Champagne, IL. The daily maximum values at Lamont, OK (station ID 74649) are also in good agreement with the wind profiler and radiosonde PBL heights computed by Simpson et al. (2007) during selected days in July 2003 over Oklahoma City, OK.

4b. PBL Heights under cloudy conditions

Algorithms to estimate PBL heights from lidar or wind profiler data have generally been restricted to clear conditions (Angevine et al., 1994, Bianco and Wilczak, 2002, Lewis et al., 2013), or have attempted to estimate PBL heights in cloudy conditions with limited success

(Bianco et al., 2008). The present WP PBL height algorithm was applied on all the mostly cloudy days during the study period at each station. The partially cloudy profiles resulted in ambiguous PBL heights, but the PBL heights for the mostly cloudy profiles were coherent.

The mean diurnal cycles under mostly cloudy (>50% cloud cover) conditions for the seven stations with RASS data are shown in Figure 8 alongside the clear sky PBL heights shown in Figure 6. At most stations, the cloudy sky PBL heights from WP, Ri_b and MERRA are in close agreement from the morning until approximately 3PM. After this time, the MERRA cloudy sky PBL heights drop while the WP and Ri_b PBL heights remain aloft. The cloudy sky PBL heights are expected to be lower than the clear sky values due to the decreased net radiation at the surface under cloudy conditions, and this is seen in all 3 PBL height estimates. The MERRA PBL heights exhibit the largest clear-cloudy difference throughout the day, with values up to 1000 m (consistent with a possible overestimate of MERRA clear sky PBL heights), the Ri_b PBL heights are generally close to 500 m, also throughout the day, and the WP PBL height difference is smallest, with values generally near 0 in the morning and closer to 250 m after 2PM.

Figure 9 shows the geographical distribution of the daily maximum clear - cloudy sky PBL height difference from the WP and MERRA estimates at the wind profiler stations in the study region. The behavior at all the stations is qualitatively the same as the behavior at the stations with RASS shown in Figure 8. That is, the MERRA clear-cloudy PBL height difference is generally quite a bit larger (by approximately 750 m) than the WP difference. WP clear-cloudy difference also shows the geographic pattern seen in the clear sky PBL heights, with a larger clear-cloudy difference in the western areas of the study region, and smaller difference in the eastern areas. This pattern stems from a more geographically uniform cloudy sky PBL height, suggesting that the cloudy sky PBL height is less sensitive to the surface temperature and moisture than the clear sky PBL height. MERRA PBL clear-cloudy PBL height difference shows little of this geographical pattern.

5. Summary and Conclusions

An algorithm was developed to compute planetary boundary layer (PBL) heights using wind profiler backscatter signal data archived by the NOAA wind profiler network. Data for this study were from June, July and August of 2000 through 2005, and the study area is the central United States. The wind profiler (WP) PBL height algorithm estimates the "emergence time" of the PBL height into the range detectable by the instrument and selects the appropriate local maximum backscatter value in each column to designate as the PBL height. WP PBL heights were evaluated under clear and cloudy conditions relative to PBL height estimates from MERRA reanalysis and from a quasi-independent estimate based on RASS temperature profiles available at a subset of the NOAA wind profiler stations using a bulk Richardson number (Ri_b) algorithm. At some stations the variation with height of the signal backscatter data does not reflect the PBL discontinuity, because of topographic variations (the 6 stations in WY, CO and NM) or due to the possible presence of aerosol layers advected from nearby (the stations at Lathrop, MO and at Wolcott, IN), and these stations were excluded from the study.

The algorithm presented here is characterized by its simplicity, in that it requires few steps and contains little site specific tuning. In addition, unlike many previous studies, the validation of the present algorithm was comprehensive, and the WP PBL heights were evaluated over a long period of time and over a wide geographic range. The robustness is largely due to the simplicity.

Clear sky mean diurnal cycles typically show the PBL emergence into instrument range occurring at approximately 10 to 11AM. The WP PBL height continues to increase to its daily maximum at approximately 4PM and levels off afterwards. WP PBL heights agree with Ri_b based PBL heights at RASS stations in the morning, are higher by approximately 250 m than the Ri_b PBL heights in the afternoon, and are lower in general than MERRA PBL heights by up to 500 m in the late afternoon. The geographical distribution of daily maximum WP PBL heights follows the expected variation with temperature and moisture, where higher PBL heights occur over warmer and drier terrain, a distribution not reflected in the MERRA PBL heights.

Cloudy sky WP PBL heights show a similar general diurnal cycle as the clear sky heights in terms of emergence time and time of daily maximum, and are generally lower than clear sky PBL heights as expected. The cloudy sky WP PBL heights are higher than both the MERRA and the Ri_b PBL heights by up to 500 m in some cases in the late afternoon. The clear-cloudy PBL height differences are smaller for the WP PBL heights than for either the Ri_b (by up to 250 m) or MERRA PBL heights (by up to 500 m), possibly reflecting an overestimate of WP cloudy sky PBL heights and an overestimate of MERRA clear sky PBL heights. The geographical distribution of the clear-cloudy difference in daily maximum PBL heights is smoother than the clear sky PBL height distribution, but also reflects the variations in temperature and moisture, where larger clear-cloudy differences occur in warmer and drier areas.

The present study has shown that existing data archives from the NOAA Profiler Network (NPN) can be used to provide reliable estimates of hourly PBL heights under clear and mostly cloudy conditions at an extensive set of locations in the central United States. Signal backscatter data are available from the NPN throughout the year, and for varying time periods at different stations. Future work will extend the temporal scope of this study to include the entire time span for each station in the wind profiler network archive, and include the analysis of annual cycles and interannual variability.

References:

Angevine, W. M., A. W. Grimsdell, L. M. Hartten,and A. C. Delany, 1998: The Flatland Boundary Layer Experiments. *Bull. Amer. Meteor. Soc.*, 79, 499-431.

Angevine, W. M., A. B. White and, S. K. Avery, 1994: Boundary-Layer Depth and Entrainment Zone Characterization with a Boundary-Layer Profiler. *Boundary Layer Meteor.*, 68, 375-385.

Ao, C. O., D. E. Waliser, S. K. Chan, J.-L. Li, B. Tian, F. Xie, and A. J. Mannucci, 2012: Planetary boundary layer heights from GPS radio occultation refractivity and humidity profiles, *J. Geophys. Res.*, 117(D16117), doi:10.1029/2012JD017598.

Beyrich, F., 1997: Mixing height estimation from sodar data – A critical discussion. *Atmos. Environ.*, 31:23, 3941-3953.

Bianco, L., J. M. Wilczak, and A. B. White, 2008: Convective Boundary Layer Depth Estimation from Wind Profilers: Statistical Comparison between an Automated Algorithm and Expert Estimations. *J. Atmos. Oceanic Tech.*, 25, 1397-1413.

Bianco, L., and J. M. Wilczak, 2002: Convective Boundary Layer Depth: Improved Measurement by Doppler Radar Wind Profiler Using Fuzzy Logic Methods. *J. Atmos. Oceanic Tech.*, 19, 1745-1758.

Bosilovich, M. G., 2013: Regional Climate and Variability of NASA MERRA and Recent Reanalyses: U.S. Summertime Precipitation and Temperature. *J. Appl. Meteor. Climatol.*, 52, 1939-1951. doi:10.1175/JAMC-D-12-0291.1.

Cohn, A. S., and W. M. Angevine, 2000: Boundary Layer Height and Entrainment Zone Thickness Measured by Lidars and Wind-Profiling Radars. *J. Appl. Meteor.*, 39, 1233–1247.

Compton, J.C., R. Delgado, T.A. Berkoff , and R. M. Hoff, 2013: Determination of Planetary Boundary Layer Height on short Spatial and Temporal Scales: A Demonstration of the Covariance Wavelet Transform in Ground-Based Wind Profiler and Lidar Measurements. *J. Atmos. Oceanic Tech.*, 30, 1566-1575.

Davis, K. J., N. Gamage, C. R. Hagelberg, C. Kiemle, D. H. Lenchow, and P. P. Sullivan, 2000: An Objective Method for Deriving Atmospheric Structure from Airborne Lidar Observations. *J. Atmos. Oceanic Tech.*, 17, 1455-1468.

Denning, A. S., T. Takahashi, and P. Friedlingstein, 2011: Can a strong atmospheric CO_2 rectifier effect be reconciled with a “reasonable” carbon budget? *Tellus B*, 51, 249-253.

Flamant, C., J. Pelon, P. H. Flamant, and P. Durand, 1997: Lidar determination of the entrainment zone thickness at the top of the unstable marine atmospheric boundary layer, *Bound.-Lay. Meteorol.*, 83, 247-284.

Federal Coordinator for Meteorological Service and Supporting Research, 1998: U. S. Wind Profilers: A Review. Technical Report, March 1998, Washington, DC. pp. 57. FCM-R14-1998.

Guo, P., Y.-H. Kuo, S. V. Sokolovskiy, and D. H. Lenschow, 2011: Estimating Atmospheric Boundary Layer Depth Using COSMIC Radio Occultation Data. *J. Atmos. Sci.*, 68, 1703–1713.

Hennemuth, B., and A. Lammert, 2006: Determination of the Atmospheric Boundary Layer Height from Radiosonde and Lidar Backscatter. *Boundary-Layer Meteor.*, 120, 181-200.

Heo, B.-H., S. Jacoby-Koaly, K.-E. Kim, B. Campistron, B. Benech, and E.-S. Jung, 2003: Use of the Doppler Spectral Width to Improve the Estimation of the Convective Boundary Layer Height from UHF Wind Profiler Observations. *J. Atmos. Oceanic Tech.*, 20, 408-424.

Hooper, W. P., and E. Eloranta, 1986: Lidar measurements of wind in the planetary boundary layer: the method, accuracy and results from joint measurements with radiosonde and kytoon. *J. Clim. Appl. Meteor.*, 25, 990-1001.

Jordan, N. S., R. M. Hoff, and J. T. Bacmeister, 2010: Validation of Goddard Earth Observing System- version 5 MERRA planetary boundary layer heights using CALIPSO. *J. Geophys. Res.*, 115, D24218, doi:10.1029/2009JD013777.

Koster, R. D., Y. C. Sud, Z. Guo, P. A. Dirmeyer, G. Bonan, K. W. Oleson, E. Chan, D. Verseghy, P. Cox, H. Davies, E. Kowalczyk, C. T. Gordon, S. Kanae, D. Lawrence, P. Liu, D.

Mocko, C.-H. Lu, K. Mitchell, S. Malyshev, B. McAvaney, T. Oki, T. Yamada, A. Pitman, C. M. Taylor, R. Vasic, and Y. Xue, 2006: GLACE: The Global Land–Atmosphere Coupling Experiment. Part I: Overview. *J. Hydrometeor.*, 7, 590-610.

Lewis, J. R., E. J. Welton, A. Molod, and E. Joseph, 2013: Improved boundary layer depth retrievals from MPLNET. *J. Geophys. Res.: Atmospheres,* 118:17, 9870-9879.

Liu, S., and X-Z. Liang, 2010: Observed Diurnal Cycle Climatology of Planetary Boundary Layer Height. *J. Climate*, 23, 5790-5809, doi:10.1175/2010JCLI3552.1.

Lammert, A., and Bösenberg, J., 2006: Determination of the Convective Boundary-Layer Height with Laser Remote Sensing. *Boundary-Layer Meteor.*, 119(1), 159-170.

McGrath-Spangler, E. L., and A. S. Denning, 2012: Estimates of North American summertime planetary boundary layer depths derived from space-borne lidar. *J. Geophys. Res.*, 117, D15, doi:10.1029/2012JD017615.

Rienecker, M. M., M. J. Suarez, R. Gelaro, R. Todling, J. Bacmeister, E. Liu, M. G. Bosilovich, S. D. Schubert, L. Takacs, G.-K. Kim , S. Bloom, J. Chen, D. Collins, A. Conaty, A. da Silva, W. Gu, J. Joiner, R. D. Koster, R. Lucchesi, A. Molod, T. Owens, S. Pawson, P. Pegion, C. R. Redder, R. Reichle, F. R. Robertson, A. G. Ruddick, M. Sienkiewicz, and J. Woollen, 2011: MERRA: NASA's Modern-Era Retrospective Analysis for Research and Applications. *J. Climate*, **24**, 3624-3648.

Rossow, W.B., A.W. Walker, D.E. Beuschel, and M.D. Roiter, 1996: International Satellite Cloud Climatology Project (ISCCP) Documentation of New Cloud Datasets. WMO/TD-No. 737, World Meteorological Organization, 115 pp. available at http://isccp.giss.nasa.gov/pub/documents/d-doc.pdf

Seibert, P., F. Beyrich, S.-E. Gryning, S. Joffre, A. Rasmussen, and P. Tercier, 2000: Review and intercomparison of operational methods for the determination of the mixing height. *Atmos. Environ.*, 34, 1001-1027.

Seidel, D. J., C. O. Ao, and K. Li, 2010: Estimating climatological planetary boundary layer heights from radiosonde observations: Comparison of methods and uncertainty analysis. *J. Geophys. Res.*, 115, D16113, doi:10.1029/2009JD013680.

Simpson M., S. Raman J.K. Lundquist, and M Leach, 2006: A study of the variation of urban mixed layer heights, *Atmos. Environ.*, 41, 6923-6930.

Singal, S. P., and M. Goel, 1997: Radio Acoustic Sounding System (RASS) for studying the lower atmosphere. Acoustic Remote Sensing Application. S. P. Singal, ed. Narosa Publishing House, New Delhi, India, 585 pp.

Spangler, T. C., and R. A. Dirks, 1974: Meso-scale variations of the urban mixing height. *Boundary-Layer Meteor.*, 6:3-4, 423-441.

Steyn, D. G., M. Baldi, and R. Hoff, 1999: The Detection of Mixed Layer Depth from Lidar Backscatter Profiles. *J. Atmos. Oceanic Tech.*, 16, 953–959.

List of Figures

Figure 1. Map of NOAA Profiler Network sites used in this study. Filled blue circles indicate wind profiler stations, filled green circles identify wind profiler stations that also have RASS. Red circles indicate the stations used to train the algorithm in this study.

Figure 2: Example of diurnal evolution of PBL height from Station 74541, Haviland, KS. (a) Shading is backscatter signal strength in dB, blue triangles are estimates of PBL height computed using the Richardson-based method and the black stars are the PBL heights from the wind profiler algorithm. (b) Vertical profiles of the wind profiler backscatter up to a height of 4000 m for every hour starting at 1PM local time.

Figure 3: Example of a discontinuous time series of PBL heights at Station 74541, from a) the wind profiler algorithm (WP) and the Richardson number based algorithm and b) from MERRA. c) Climatological diurnal cycle for all three estimates. Units of PBL height are m.

Figure 4: a) Variance of topographic height at scales less than 3 km in m^2. b) diurnal evolution of PBL height from Station 74629, White Sands, NM. Shading is backscatter signal strength in dB, black stars are the PBL heights from the wind profiler algorithm. c) Vertical profiles of the wind profiler backscatter for the same location as b) up to a height of 4000 m for every hour starting at 1PM local time.

Figure 5: Examples of diurnal evolution of PBL height from Station 74551, Lathrop, MO. (a) Sample clear day's data. Shading is backscatter signal strength in dB, black stars are the PBL heights from the wind profiler algorithm. (b) Vertical profiles of the wind profiler backscatter up to a height of 4000 m for every hour starting at 1PM local time. c) same as a) but for a cloudy day. d) same as b) but for a cloudy day.

Figure 6: Climatological diurnal cycles of wind profiler (red), Richardson number (green) and MERRA (blue) estimates of PBL height in m under clear conditions for the 7 stations with RASS. Station numbers correspond to the labels in Figure 1. a) Station 74541, b) Station 74542, c) Station 74546, d) Station 74648, e) Station 74735, f) Station 74640, g) Station 74649.

Figure 7: Geographical distribution of daily maximum PBL height under clear sky conditions in m from a) wind profiler estimate and b) MERRA estimate.

Figure 8: Climatological diurnal cycles of wind profiler (red), Richardson number (green) and MERRA (blue) estimates of PBL height in m under clear conditions (solid lines) conditions of greater than 50% cloud cover for the 8 stations with RASS. Station numbers correspond to the labels in Figure 1. a) Station 74541, b) Station 74542, c) Station 74546, d) Station 74648, e) Station 74735, f) Station 74640, g) Station 74649.

Figure 9: Geographical distribution of daily maximum clear sky PBL height minus daily maximum cloudy PBL height in m from a) wind profiler estimate and b) MERRA estimate.

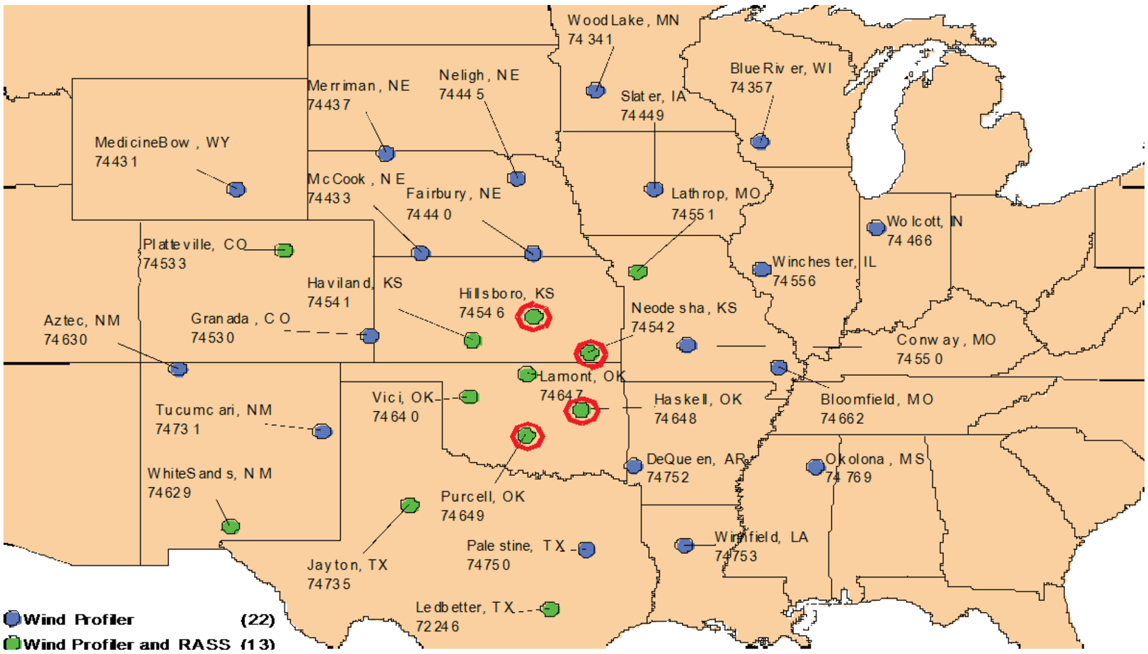

Figure 1. Map of NOAA Profiler Network sites used in this study. Filled blue circles indicate wind profiler stations, filled green circles identify wind profiler stations that also have RASS. Red circles indicate the stations used to train the algorithm in this study.

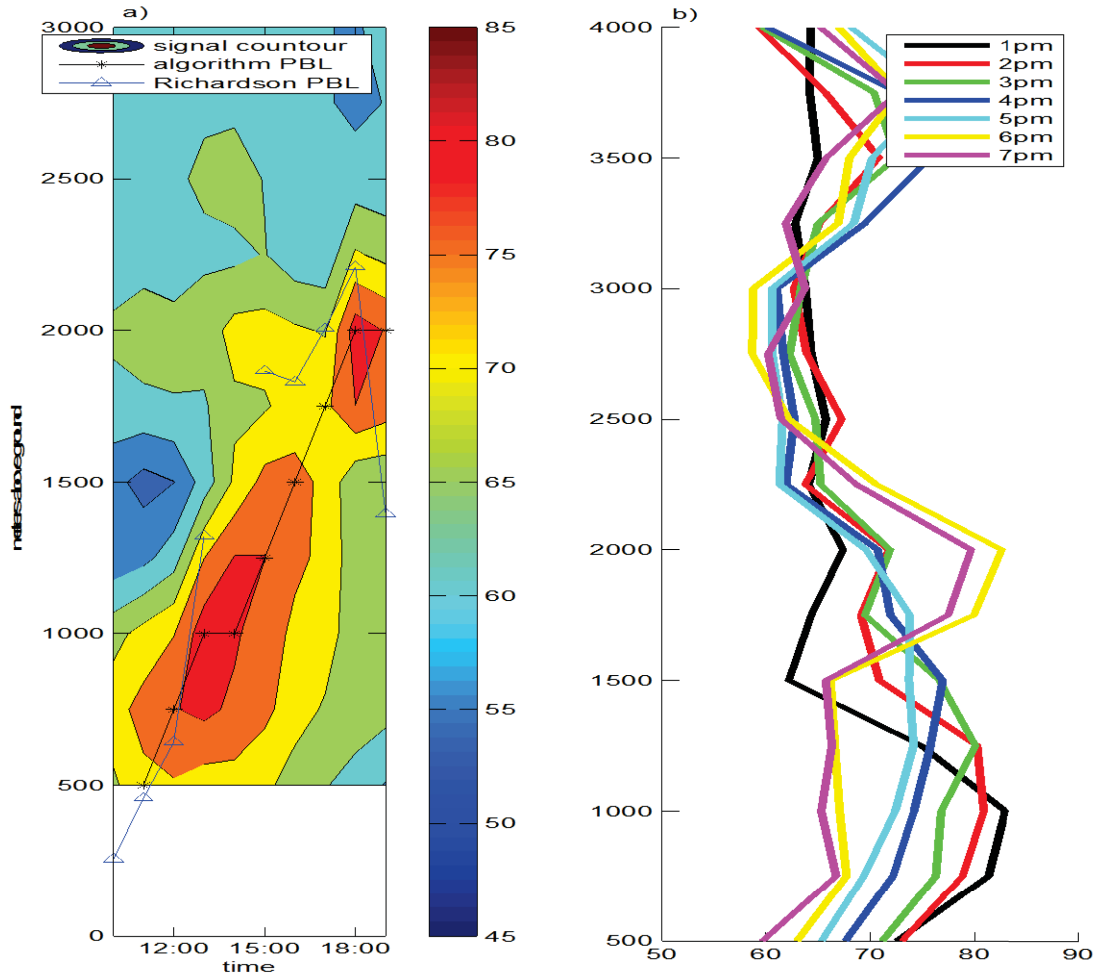

Figure 2: Example of diurnal evolution of PBL height from Station 74541, Haviland, KS. a) Shading is backscatter signal strength in dB, blue triangles are estimates of PBL height computed using the Richardson-based method and the black stars are the PBL heights from the wind profiler algorithm. b) Vertical profiles of the wind profiler backscatter up to a height of 4000 m for every hour starting at 1PM local time.

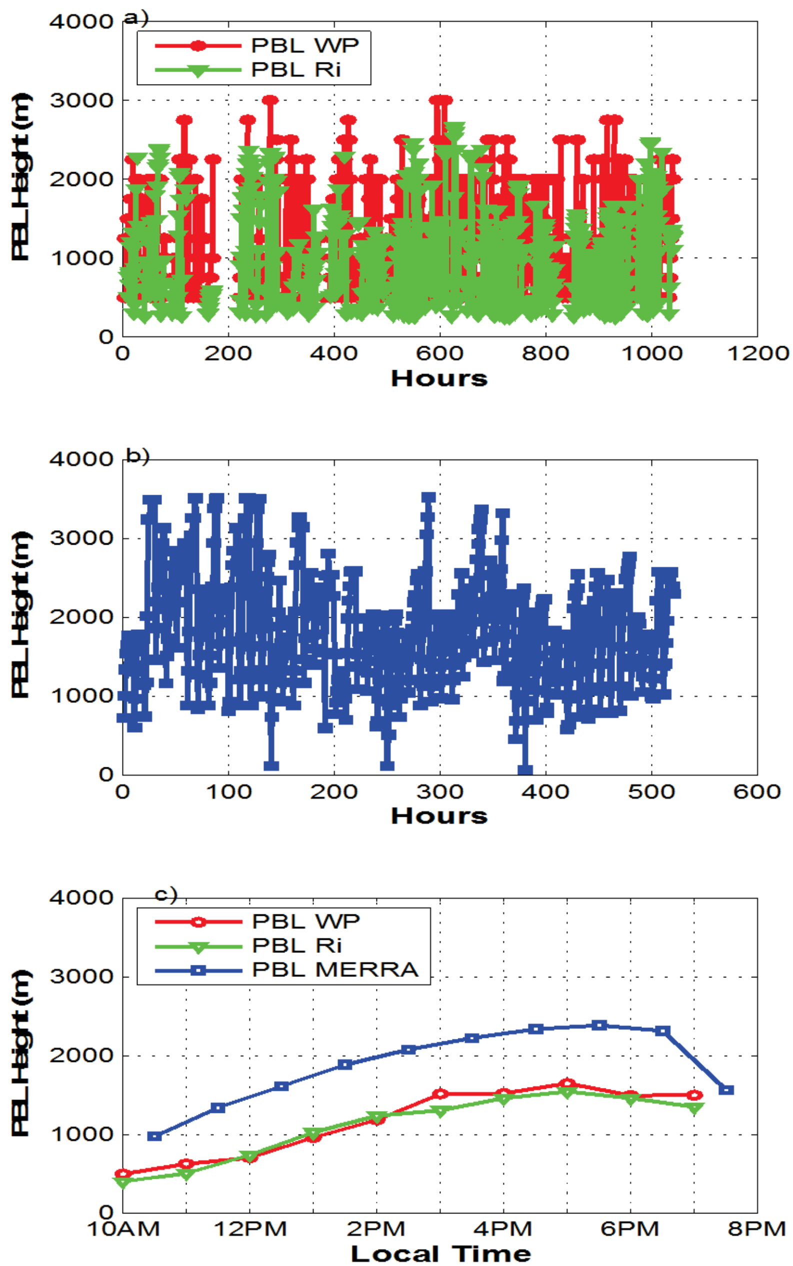

Figure 3: Example of a discontinuous time series of PBL heights at Station 74541, from a) the wind profiler algorithm (WP) and the Richardson number (Ri) based algorithm and b) from MERRA. c) Climatological diurnal cycle for all three estimates. Units of PBL height are m.

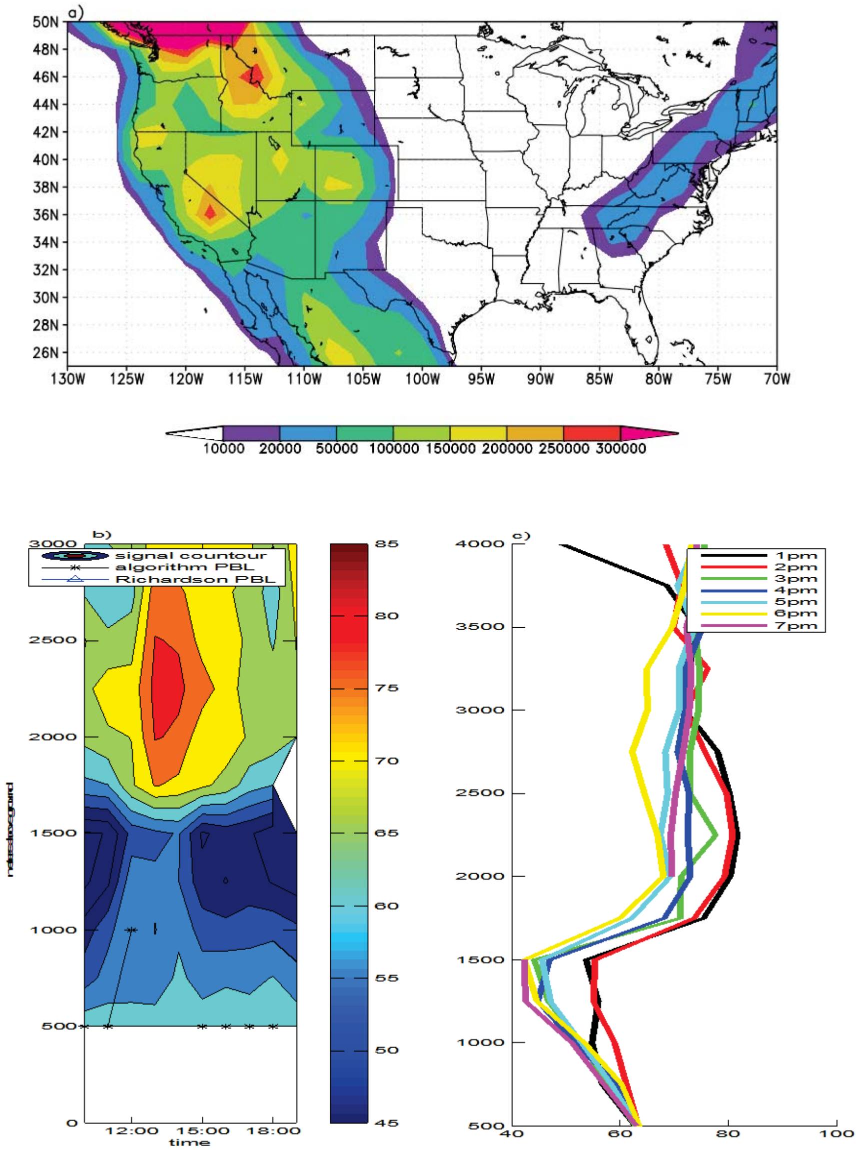

Figure 4: a) Variance of topographic height at scales less than 3 km in m2. b) diurnal evolution of PBL height from Station 74629, White Sands, NM. Shading is backscatter signal strength in dB, black stars are the PBL heights from the wind profiler algorithm. c) Vertical profiles of the wind profiler backscatter for the same location as b) up to a height of 4000 m for every hour starting at 1PM local time.

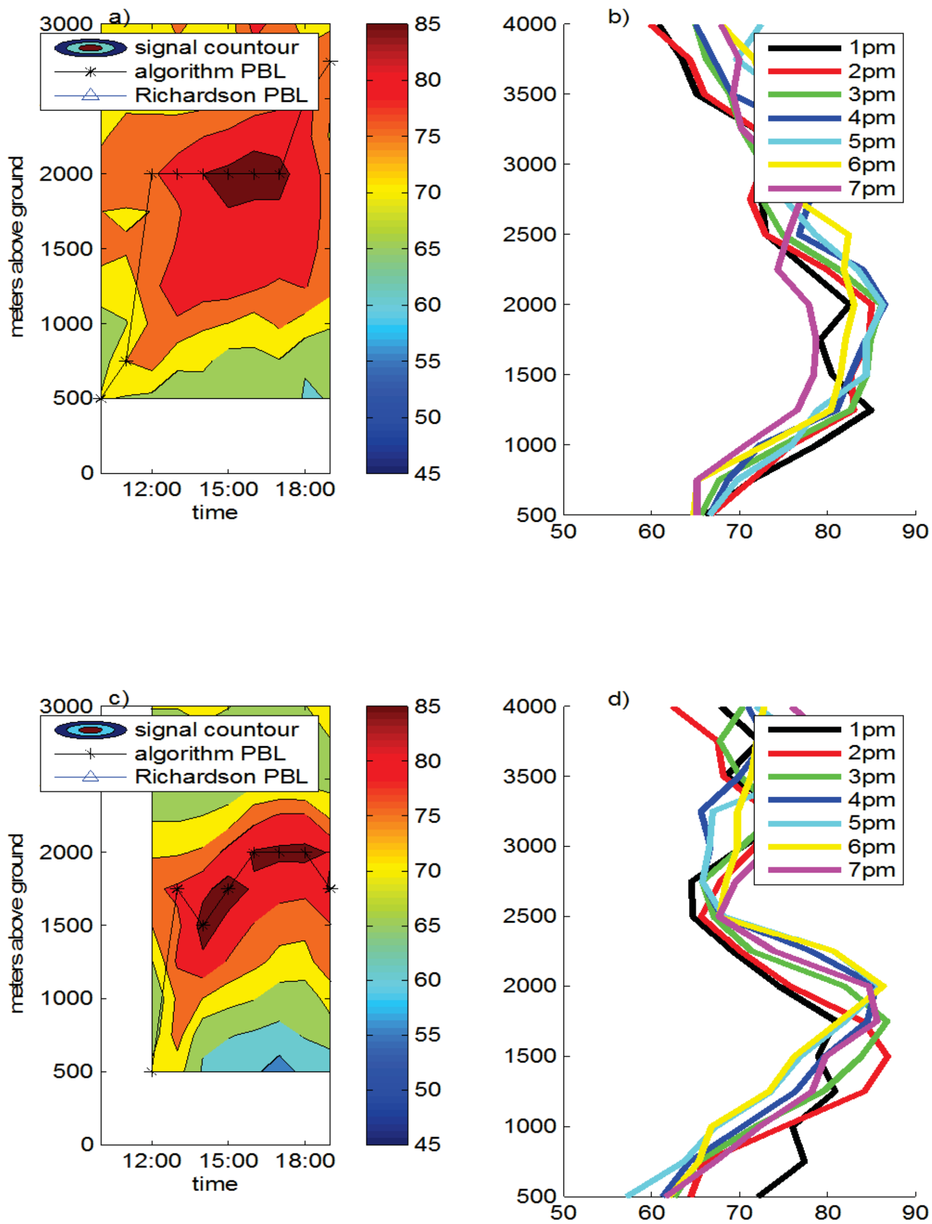

Figure 5: Examples of diurnal evolution of PBL height from Station 74551, Lathrop, MO. (a) Sample clear day's data. Shading is backscatter signal strength in dB, black stars are the PBL heights from the wind profiler algorithm. (b) Vertical profiles of the wind profiler backscatter up to a height of 4000 m for every hour starting at 1PM local time. c) same as a) but for a cloudy day. d) same as b) but for a cloudy day.

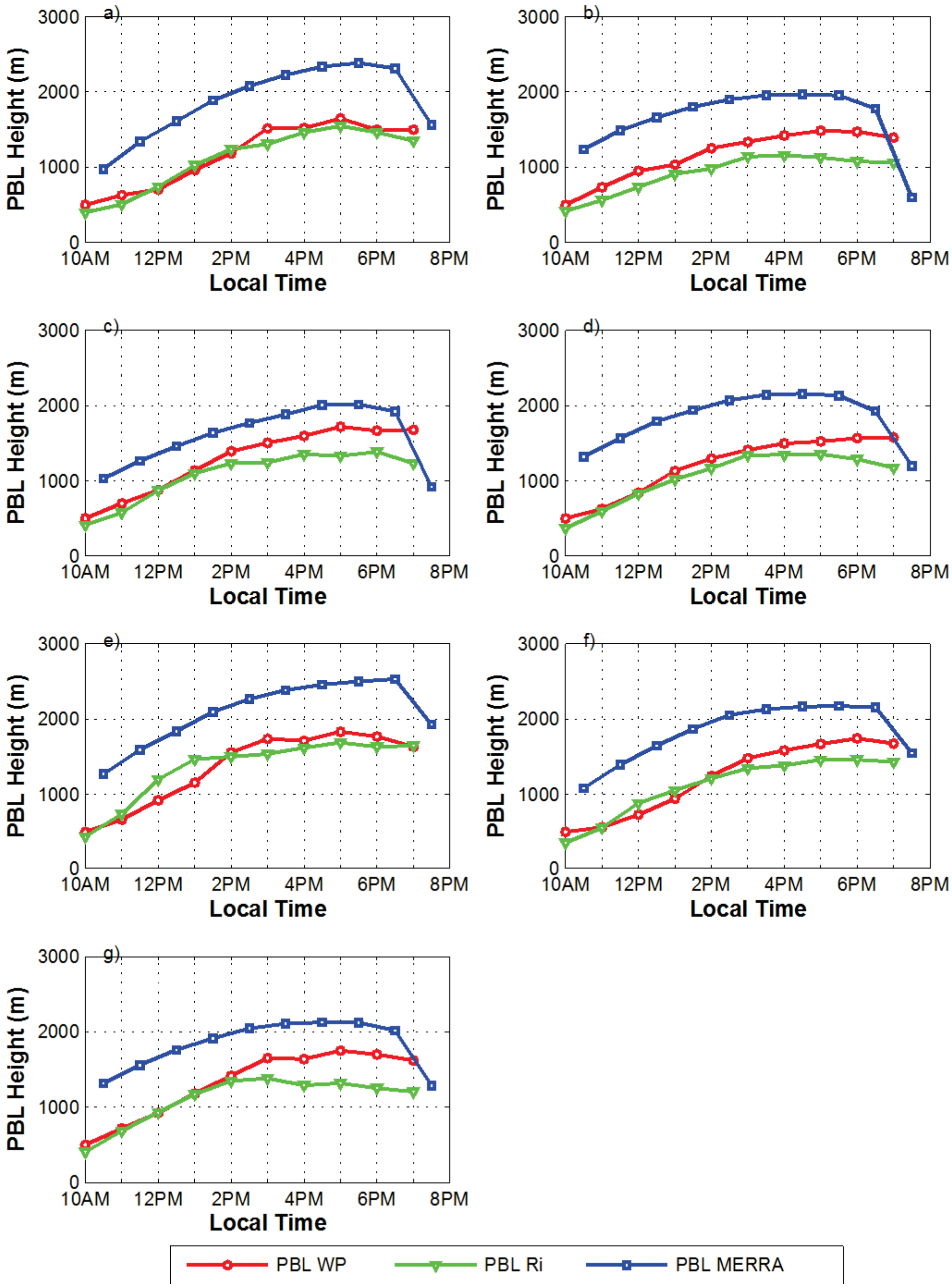

Figure 6: Climatological diurnal cycles of wind profiler (red), Richardson number (green) and MERRA (blue) estimates of PBL height in m under clear conditions for the 8 stations with RASS. Station numbers correspond to the labels in Figure 1. a) Station 74541, b) Station 74542, c) Station 74546, d) Station 74648, e) Station 74735, f) Station 74640, g) Station 74649.

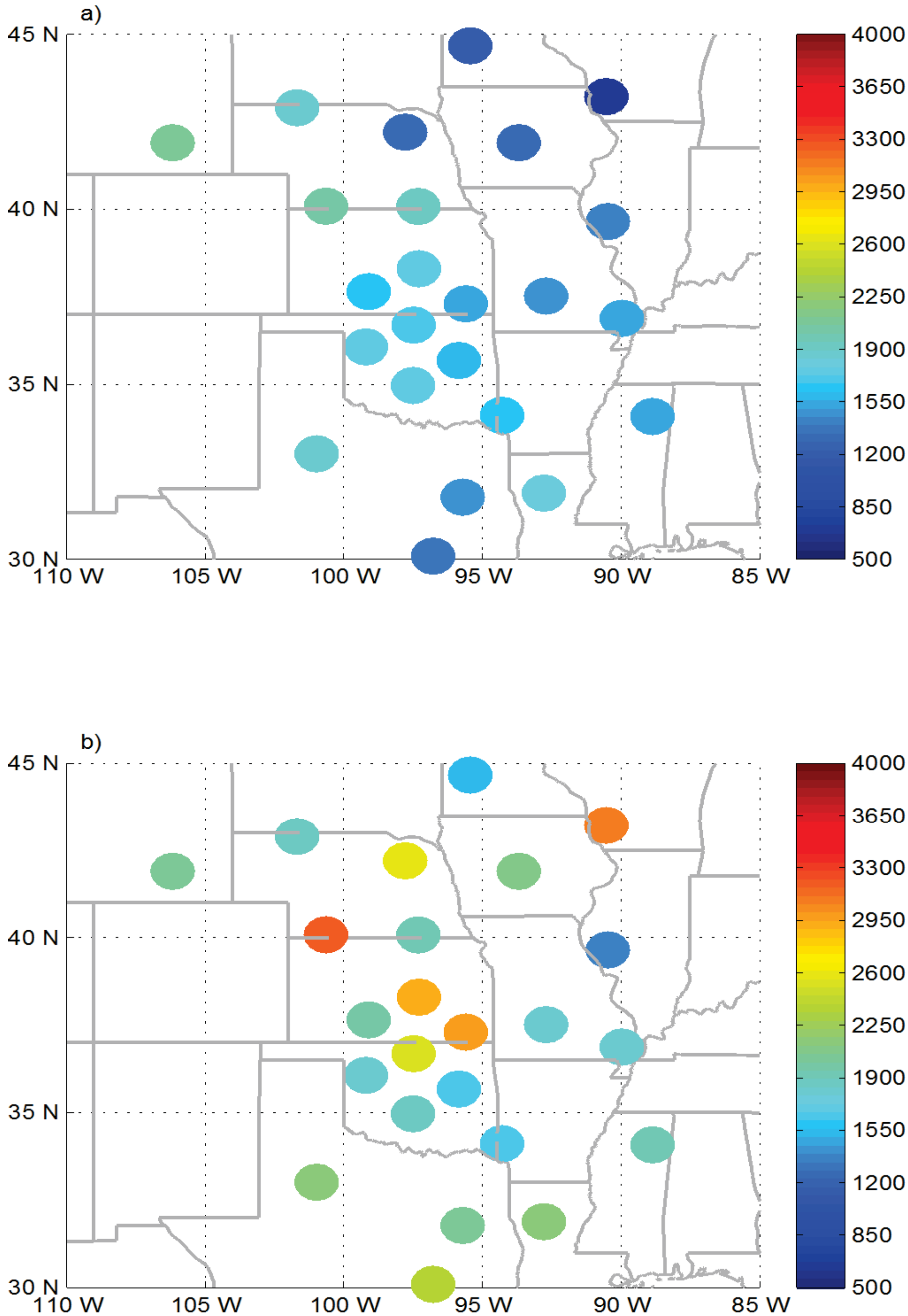

Figure 7: Geographical distribution of daily maximum PBL height under clear sky conditions in m from a) wind profiler estimate and b) MERRA estimate.

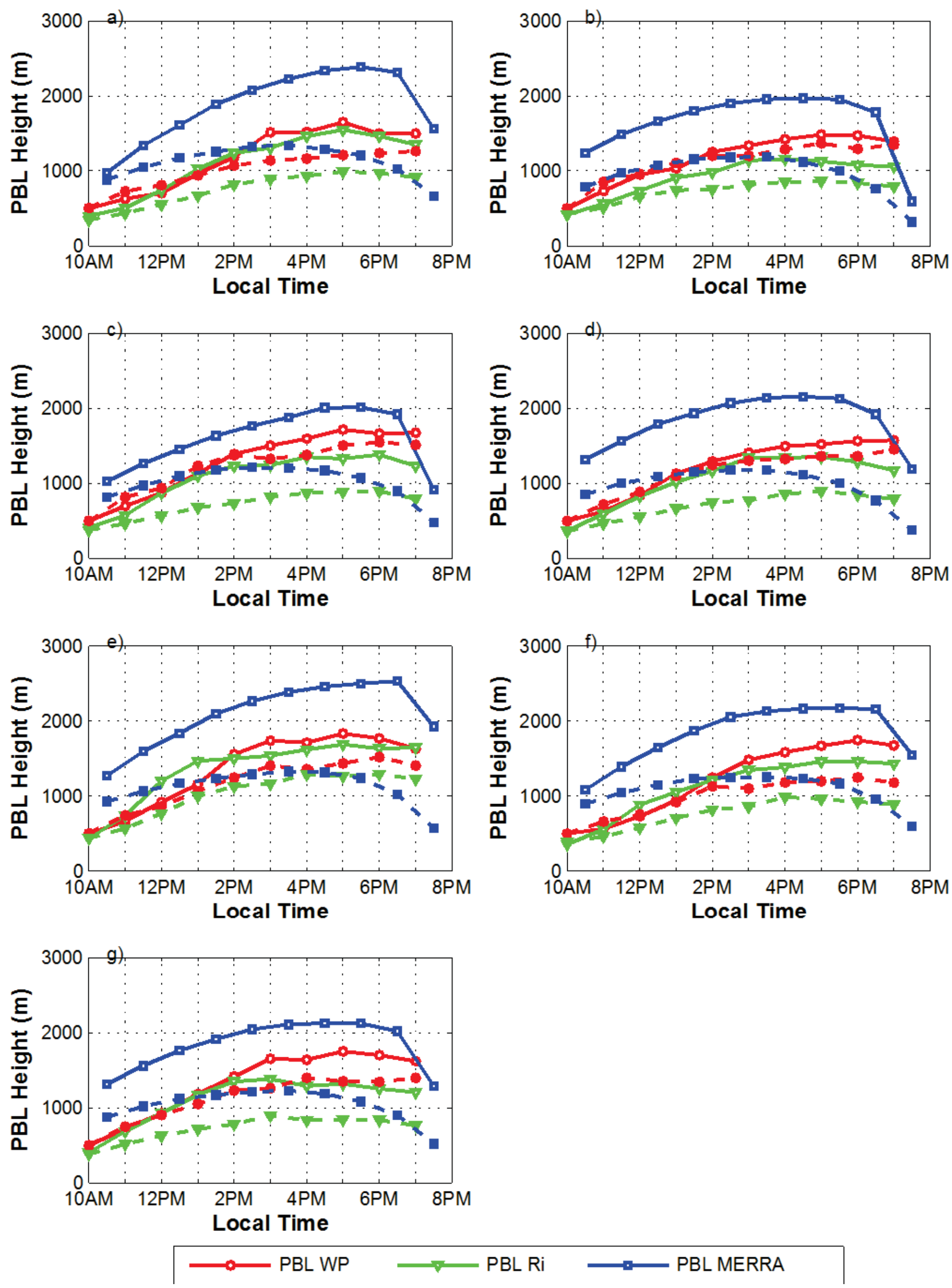

Figure 8: Climatological diurnal cycles of wind profiler (red), Richardson number (green) and MERRA (blue) estimates of PBL height in m under clear conditions (solid lines) conditions of greater than 50% cloud cover for the 8 stations with RASS. Station numbers correspond to the labels in Figure 1. a) Station 74541, b) Station 74542, c) Station 74546, d) Station 74648, e) Station 74735, f) Station 74640, g) Station 74649.

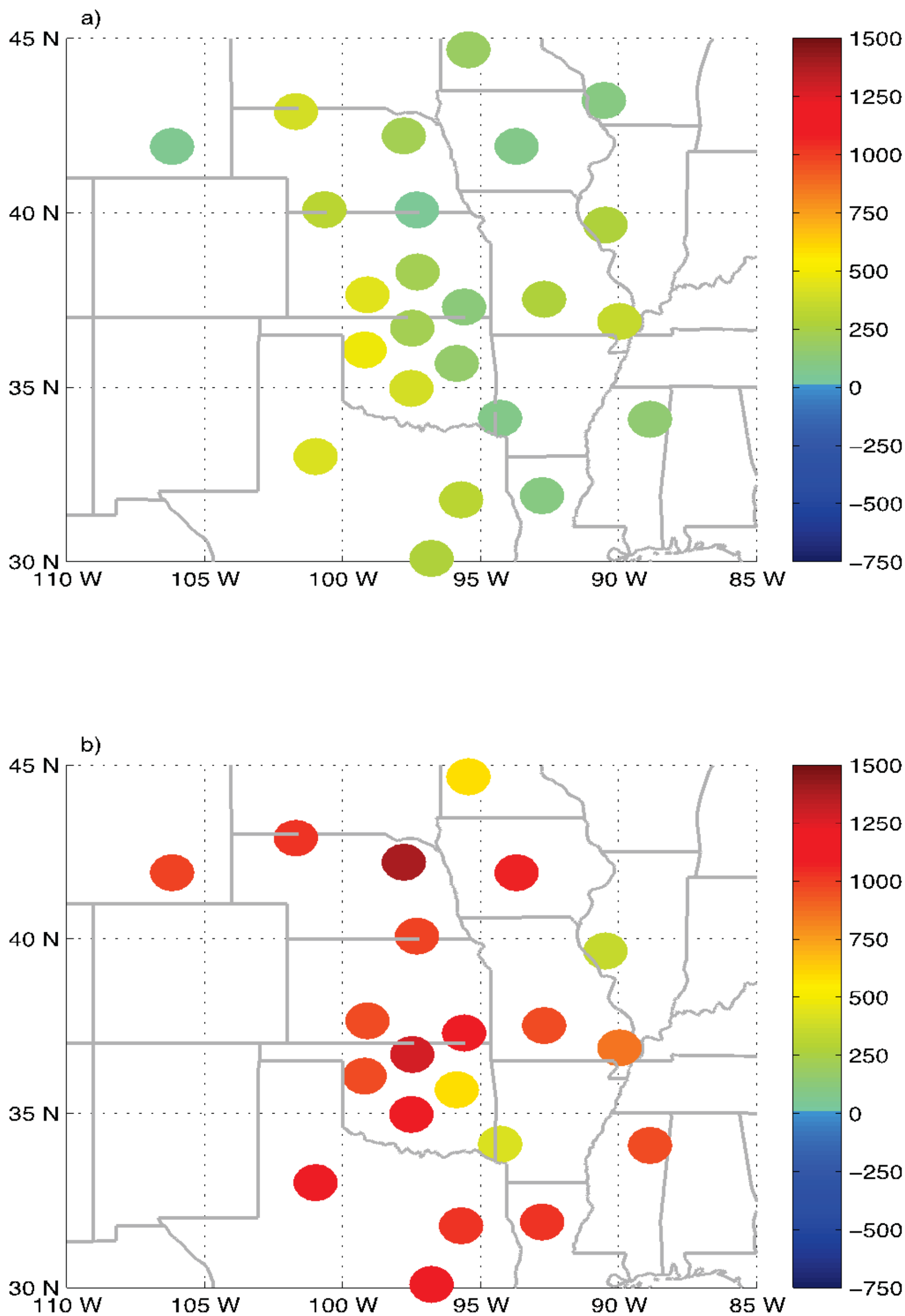

Figure 9: Geographical distribution of daily maximum clear sky PBL height minus daily maximum cloudy PBL height in m from a) wind profiler estimate and b) MERRA estimate.